Simple compact Fizeau wavemeter

D. F. Gray, K. A. Smith, and F. B. Dunning

A relatively simple, inexpensive, and compact Fizeau wavemeter is described that provides an accuracy of better than 1 part in 10^6 across the visible spectrum. The design is a variant of that initially proposed by Gardner and employs a novel geometry to eliminate wavelength measurement errors due to changes in wave front curvature.

With the increased use of tunable lasers has come the need for instruments to measure rapidly and accurately their output wavelengths. A number of wavemeters, based on a variety of different operating principles, have been described in the literature.[1–16] Instruments that make use of a Fizeau wedge interferometer[1–3,16] have the advantage that they can be used with both pulsed and cw laser sources. Typically, a Fizeau interferometer is formed using two uncoated optical flats inclined at a small angle so that their inner faces form a thin wedge of angle α. The reflection of plane monochromatic radiation from these faces results in formation of a series of uniformly spaced interference fringes that are parallel to the wedge axis. For incident radiation of wavelength λ, the intensity in the perpendicular y direction is proportional to

$$I(y) \propto \left[1 + \cos\left(\frac{2\pi}{\Lambda} y + \phi\right)\right], \tag{1}$$

where $\Lambda = \lambda/2\alpha$ is the fringe spacing, and ϕ is the phase at $y = 0$. In a Fizeau wavemeter, the fringe spacing and phase of the interference pattern are typically measured using a linear photodiode array. This, coupled with accurate calibration of the wedge angle and spacing, enables the input wavelength to be precisely determined. In the present paper we describe a relatively inexpensive, simple, and compact Fizeau wavemeter that is a variant of a design initially proposed by Gardner.[16] This instrument provides an accuracy of better than 1 part in 10^6 across the visible spectrum.

One important consideration in the design of a Fizeau wavemeter is to ensure that changes in the curvature of the wave front incident on the wedge do not lead to errors in the measured wavelengths. In earlier Fizeau wavemeter designs,[1–3] the sensitivity to wave front curvature has been minimized by tilting the wedge and placing the photodiode array at a point of zero shear, typically ~0.4 m from the wedge. Gardner[16] pointed out, however, that effects due to wave front curvature can be made negligibly small by tilting the wedge so that the radiation is incident, at some angle of incidence θ, in a plane normal to the wedge and parallel to the wedge axis, and placing the photodiode array within ~10 mm of the wedge. This approach was adopted in the present design, although mechanical considerations, in particular the size of the evacuated enclosure in which the Fizeau wedge is located, dictated that the photodiode array must be at least 30 mm from the wedge. To evaluate the potential and performance of such an instrument, and its sensitivity to wave front curvature, the simple model illustrated in Fig. 1 was used. The faces of the wedge are labeled F_1 and F_2. The model assumes spherical wave front curvature, and Fig. 1 is drawn for the case where the incident wave front has positive curvature. Interference effects are discussed in terms of radiation from a point source S located a perpendicular distance s from F_1. The images of S formed in F_1 and F_2 are labeled S_1 and S_2, respectively, and provide two coherent sources of radiation. The photodiode array lies in a plane-parallel to F_1 at a perpendicular distance d. The fringe spacing at the photodiode array is determined by computing the optical path difference between rays from S_1 and S_2 at points along the array. The coordinate system used for these calculations is indicated in Fig. 1. The x-y plane is parallel to F_1 and contains the photodiode array. The x and y axes are parallel and perpendicular, respectively, to the wedge axis. S is assumed to lie in the $y = 0$ plane. The origin of the x coordinate is taken to be that point on the x axis midway between the point of intersection of a ray, incident in the $y = 0$ plane at an angle θ, reflected from F_1 and the projection on the x axis of a similar ray reflected from F_2. Geometrical considerations show

The authors are with Rice University, Houston, Texas 77251.
Received 25 November 1985.
0003-6935/86/081339-05$02.00/0.

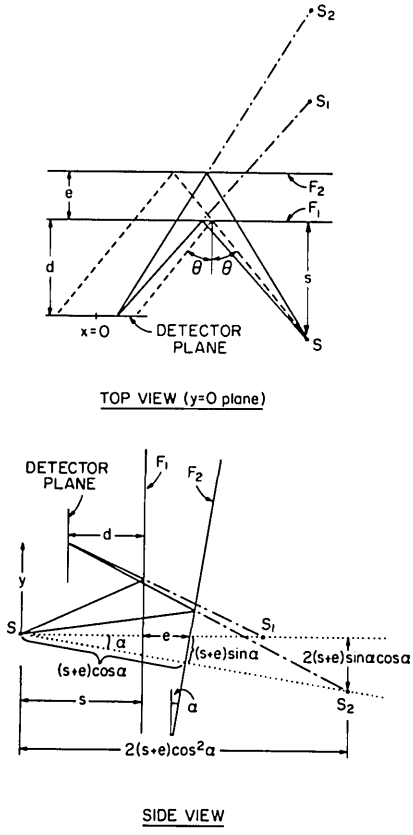

Fig. 1. Geometry used to evaluate the performance of the wavemeter.

that the path lengths from S_1 and S_2 to a point P on the photodetector array may be written

$$S_1P = \{(s+d)^2 + y^2 + [(s+d+e)\tan\theta - x]^2\}^{1/2},$$
$$S_2P = \{[2(s+e)\cos^2\alpha - (s-d)]^2 + [y + (s+e)\sin 2\alpha]^2 + [(s+d+e)\tan\theta - x]^2\}^{1/2}, \quad (2)$$

where x and y are the coordinates of the point P, and e is the separation of F_1 and F_2 at $y = 0$. Optical path differences (OPDs) at points along the array derived using these expressions are used to compute the expected phase and periodicity of the interference pattern.

To investigate effects due to wave front curvature, s is varied while keeping the angle θ constant. Although preliminary calculations indicated that the sensitivity to wave front curvature decreases with both d and θ, practical considerations dictated that these parameters have the minimum values $d = 30$ mm and $\theta = 15°$. These values were used to obtain the results discussed here. A wedge spacing $e = 1.1$ mm was chosen for the present instrument as this provides order numbers of ~4000 permitting measurements with visible input radiation having linewidths up to ~0.5 Å. A wedge angle $\alpha = 3.8'$ was selected because this leads to a convenient fringe spacing. Calculations using these values of d, θ, e, and α showed that changes in wave front curvature result in significant changes in the spacing of the interference fringes along the y axis.

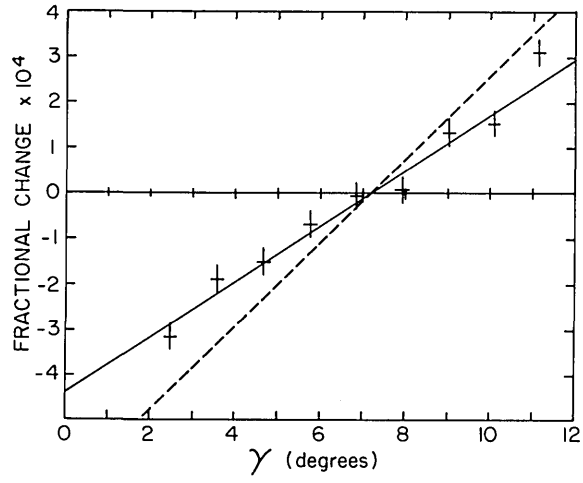

Fig. 2. Fractional change in fringe spacing that results from changing the wave front curvature from 10^5 to 50 m, - - -, and from 150 to 50 m, —, as a function of the angle γ between the y axis and the photodiode array. The experimental data + are for a change from 150 to 50 m.

Thus, if the photodiode array is aligned along the y axis, the measured fringe spacing will be sensitive to wave front curvature. Further calculations demonstrated, rather surprisingly, that this sensitivity could be made extremely small by rotation of the photodiode array in the x-y plane. This is illustrated, assuming an input wavelength of 514.5 nm, in Fig. 2, which shows the fractional change in the measured fringe spacing that results from changing s from 10^5 to 50 m, and from 150 to 50 m, as a function of the angle γ between the y axis and the photodiode array. The midpoint of the array is assumed to remain fixed at the origin $x = y = 0$. It is apparent that sizable changes in wave front curvature during operation with $\gamma \sim 7°$ will result in only very small changes in the measured fringe spacing, i.e., in only very small changes in the OPDs at points along the array. Indeed, near the center of the array, the calculated change in the OPD is $\ll 1$ Å. Thus changes in wave front curvature will not lead to a significant change in the phase of the measured interference pattern. The case of negative incident wave front curvature can be investigated using negative values of s in Eqs. (2). Sensitivity to changes in wave front curvature is minimized by operation with the same rotation angle, $\gamma \sim 7°$, as for positive wave front curvature.

The present wavemeter is shown schematically in Fig. 3. The input beam is focused on a 6-μm diam spatial filter and collimated using a 300-mm focal length achromatic lens. A portion of the collimated output is selected by a rectangular beam mask and illuminates the Fizeau wedge, the separation of which is maintained by low-expansion Zerodur spacers. To eliminate effects associated with changes in atmospheric pressure and humidity, the wedge is mounted in a sealed enclosure, equipped with optically flat windows, that is evacuated to 10^{-2} Torr. The temperature of the enclosure is controlled to ±0.5°C to minimize errors due to thermal expansion of the wedge. The radiation is incident, in a plane normal to the

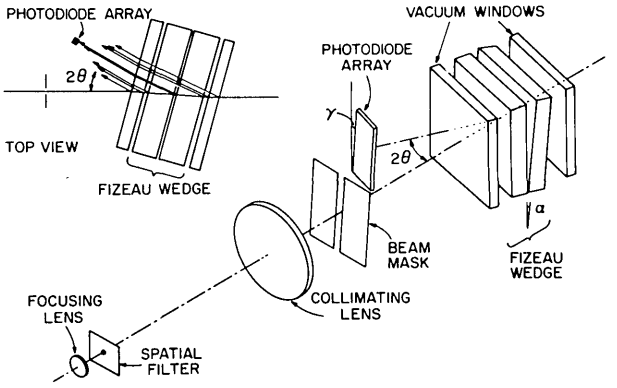

Fig. 3. Schematic diagram of the wavemeter.

wedge and parallel to the wedge axis, at an angle of incidence $\theta = 15°$. As illustrated to the inset in Fig. 3, the beams reflected from the wedge are spatially separated from those reflected at other faces. The position of the beams reflected from the wedge changes slightly with wavelength due to dispersion effects, but calculations using the model described earlier showed that this will not lead to significant measurement errors. The interference pattern is recorded using a Reticon RL 1024H linear photodiode array that is interfaced to a PDP LSI 11/23 microcomputer. The photodiode array has 1024 elements with a spacing of 15 μm and, depending as to the input wavelength, encompasses ~50–75 interference fringes. The array is in a plane parallel to the wedge and oriented with the line of diodes at an angle $\gamma = 7°$ to the y (vertical) axis. To accurately position the photodiode array, a pinhole is placed at the center of the collimating lens, and the array is centered on the reflections from the faces of the wedge. The periodicity and phase of the interference pattern are determined using the procedure described by Snyder.[2,17] In preliminary investigations, a more sensitive Texas Instruments TC101 photodetector array was used. This is a CCD device that employs MOS capacitors as sensors. Use of this device was discontinued, however, because spurious interference effects originating within the device itself complicated interpretation of the Fizeau fringe pattern. These effects, which presumably result from reflections from the semitransparent thin-film electrodes that overlay the sensor elements, are evident in Fig. 4, which shows under identical conditions segments of the interference patterns as recorded using the CCD and photodiode arrays.

In initial experiments, the sensitivity to changes in wave front curvature was explored. For these measurements, the radius of curvature of the output wave front from the collimating lens was first maximized (to $\gtrsim$300 m) using a shearing plate interferometer.[18] Other radii of curvature were obtained by translating the collimating lens from its optimum position through a distance calculated to yield the desired radius of curvature. The observed change in fringe spacing that results from changing the wave front curvature from 150 to 50 m is shown in Fig. 2 as a function of

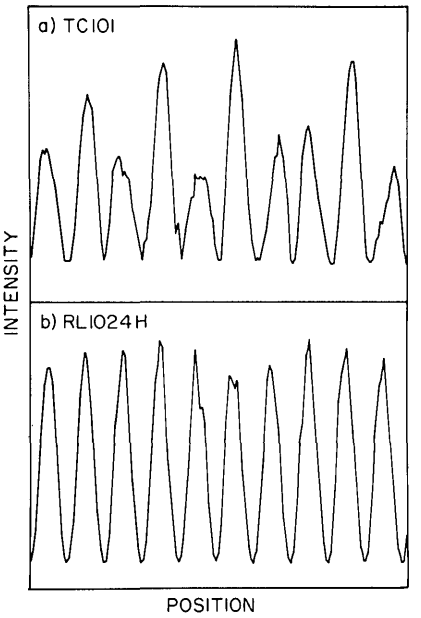

Fig. 4. Comparison of interference fringes as recorded under identical conditions using (a) the CCD array and (b) the photodiode array.

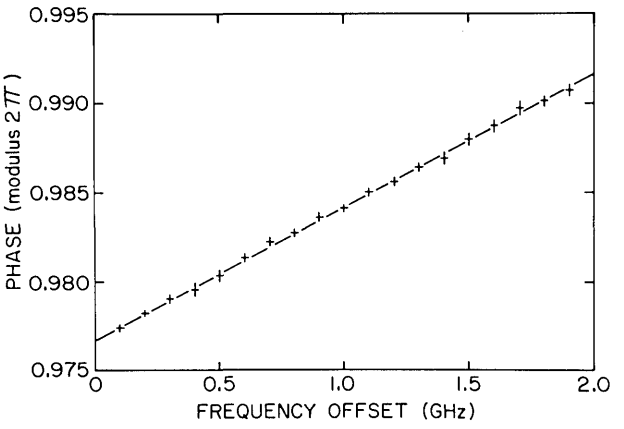

Fig. 5. Phase of the interference pattern expressed as a fraction of 2π as a function of relative input frequency.

γ. A clear minimum in the sensitivity to wave front curvature is evident for $\gamma \sim 7°$, and the data are in good agreement with the model predictions.

The resolution of the wavemeter was investigated using a single-mode frequency-stabilized Coherent model CR-699-21 ring dye laser. In these experiments the phase of the interference pattern at a fixed reference point at the center of the photodiode array was measured as the laser control electronics were used to step the laser output frequency over a range of 2 GHz. The data, shown in Fig. 5, demonstrate that frequency shifts of $\lesssim$125 MHz, i.e., ~2–3 parts in 10^7, can be resolved with the present instrument.

The instrument was calibrated using output lines from an argon-ion laser and a He–Ne laser. These two lasers provide a total of eleven lines spanning the 455–633-nm wavelength range. Although the available lasers had only short cavities, and thus relatively

large mode spacings, it is assumed that the center of gravity of each output line is fixed and equal to the accurately known wavelengths of the corresponding transitions. Measurements of the periodicity of the interference fringes at each calibration wavelength demonstrated that, as expected, the fringe spacing is proportional to the input wavelength and provided the corresponding constant of proportionality κ. These measurements further demonstrate that the fringe spacings are insensitive to the small changes in wave front curvature that result from chromatic effects associated with the collimating lens. Given κ, it is possible to obtain an approximate value for any input wavelength simply by determining the corresponding fringe spacing. More accurate wavelength determinations, however, also require measurement of the phase of the interference pattern at a fixed reference point near the center of the array for which the corresponding OPD is precisely known. This latter quantity can, in principle, be determined by careful measurement of the phase of the interference pattern at the reference point for each calibration wavelength and finding, by iteration, the OPD that correctly predicts all the measured phases. Application of this technique is complicated in the present work because, for historical reasons, the optical flats forming the Fizeau wedge are themselves wedged (by ~0.5°) and oriented so that their wedge axes are perpendicular to that of the Fizeau wedge. This introduces an additional OPD between the interfering rays and also gives rise to a small deviation of the incident beam, which changes the angle of incidence θ at the Fizeau wedge. Because of dispersion, both OPD and deviation, i.e., θ, depend on wavelength, and this results in a systematic wavelength-dependent shift in the phase of the interference patterns and in a change in fringe spacing. Calculations indicated that the resultant change in fringe spacing is negligible. The phase shifts introduced by dispersive effects, while relatively small, are not negligible. To a first approximation, however, the phase shift will vary linearly with wavelength in the visible because of the near-linear wavelength dependence of the refractive index of quartz and the small angle changes involved. The following procedure was, therefore, adopted to determine the OPD corresponding to the reference point and the wavelength dependence of the systematic phase shift. The phase of the interference pattern at the reference point was precisely measured for each calibration wavelength. An OPD equal to the approximately known wedge spacing was assumed and used to calculate the phases expected for each calibration wavelength. The residual phase differences between the calculated and measured phases were then computed and their wavelength dependence fit to a straight line. The OPD was then systematically varied to optimize the fit of the residual phase differences to a straight line. The result of such an optimization is shown in Fig. 6. A linear dependence in the residual phase differences that result from phase shifts introduced by dispersion is clearly evident. Following correction for this systematic effect, the phase difference

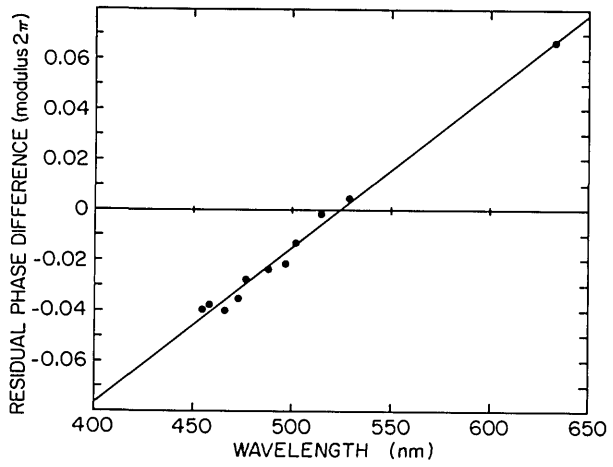

Fig. 6. Wavelength dependence of the residual phase differences that remain following optimization of the OPD corresponding to the fixed reference point.

(expressed as a fraction of 2π) between the measured and calculated phases at each calibration wavelength is $\lesssim 0.004$. Such phase differences correspond to wavelength measurement errors of <1 part in 10^6.

To determine an unknown wavelength, the periodicity of the interference pattern is measured together with the phase at the reference point. An approximate wavelength is derived from the fringe spacing. The known OPD corresponding to the reference point is divided by this approximate wavelength to obtain the order number and an approximate phase. This phase is then replaced by the measured phase, corrected for the wavelength-dependent phase shift discussed previously, and the accurate wavelength is obtained by dividing the OPD by this corrected quantity, i.e., the order number plus phase (expressed as a fraction of 2π).

The wavemeter is applied to measure the output wavelength of a single-mode frequency-stabilized rhodamine 6G ring dye laser. This laser is used to excite potassium or rubidium atoms in a collimated beam to high-Rydberg states by transverse two-photon excitation. Because the positions of alkali Rydberg levels are precisely known,[19] the wavemeter permits the laser to be rapidly tuned to excite a particular Rydberg state. The differences between the measured and known excitation wavelengths provide a direct test of the performance of the instrument and demonstrate that it can be used to measure wavelengths to an abolute accuracy of better than 1 part of 10^6.

This research is supported by the National Science Foundation under grant PHY84-05945 and the Robert A. Welch Foundation.

References

1. A number of wave meter designs are discussed in J. L. Hall and J. L. Carlsen, Eds., *Laser Spectroscopy III* (Springer-Verlag, Berlin, 1977); see also J. J. Snyder, "Laser Wavelength Meters," Laser Focus **18,** 55 (1982).
2. M. B. Morris, T. J. McIlrath, and J. J. Snyder, "Fizeau Wavemeter for Pulsed Laser Wavelength Measurement," Appl. Opt. **23,** 3862 (1984).
3. J. J. Snyder, "Fizeau Wavemeters," Proc. Soc. Phot.-Opt. Instrum. Eng. **288,** 258 (1981).
4. F. Docchio, F. P. Schäfer, J. Jethwa, and J. Jasny, "A Wavelength Meter Based on a Rotating Parallelepiped Interferometer," J. Phys. E **18,** 849 (1985).
5. P. Juncar and J. Pinard, "A New Method for Frequency Calibration and Control of a Laser," Opt. Commun. **14,** 438 (1975).
6. N. Pelletier-Allard and R. Pelletier, "Simple and Inexpensive Laser Wavelength Calibration System with a 0.01 Å Accuracy over all the Visible Range," Rev. Sci. Instrum. **55,** 1442 (1984).
7. A. Fischer, R. Kullmer, and W. Demtröder, "Computer Controlled Fabry-Perot Wavemeter," Opt. Commun. **39,** 277 (1981).
8. N. Konishi, T. Suzuki, Y. Taira, H. Kato, and T. Kasuya, "High Precision Wavelength Meter with Fabry-Perot Optics," Appl. Phys. **25,** 311 (1981).
9. R. Salimbeni and R. V. Pole, "Compact High-Accuracy Wavemeter," Opt. Lett. **5,** 39 (1980).
10. J.-P. Monchalin *et al.*, "Accurate Laser Wavelength Measurement with a Precision Two-Beam Scanning Michelson Interferometer," Appl. Opt. **20,** 736 (1981).
11. H. R. Xia, S. V. Benson, and T. W. Hänsch, "A 'Toy-Train' Wavemeter," Laser Focus **17,** 54 (1981).
12. S. J. Bennett and P. Gill, "A Digital Interferometer for Wavelength Measurement," J. Phys. E **13,** 174 (1980).
13. J. Cachenaut, C. Man, P. Cerez, A. Brillet, F. Stoeckel, A. Jourdan, and F. Hartmann, "Description and Accuracy Tests of an Improved Lambdameter," Rev. Phys. Appl. **14,** 685 (1979).
14. J. L. Hall and S. A. Lee, "Interferometric Real Time Display of CW Dye Laser Wavelength with sub-Doppler Accuracy," Appl. Phys. Lett. **29,** 367 (1976).
15. F. V. Kowalski, R. T. Hawkins, and A. L. Schawlow, "Digital Wavemeter for cw Lasers," J. Opt. Soc. Am. **66,** 965 (1976).
16. J. L. Gardner, "Wave-front Curvature in a Fizeau Wavemeter," Opt. Lett. **8,** 91 (1983); "Compact Fizeau Wavemeter," Appl. Opt. **24,** 3570 (1985).
17. J. J. Snyder, "Algorithm for Fast Digital Analysis of Interference Fringes," Appl. Opt. **19,** 1223 (1980).
18. M. V. R. K. Murty, "Lateral Shearing Interferometers," in *Optical Shop Testing*, D. Malacara, Ed. (Wiley, New York, 1978), pp. 105–148.
19. C. J. Lorenzen and K. Niemax, "Quantum Defects of the $n^2P_{1/2,3/2}$ Levels in ^{39}KI and ^{85}RbI," Phys. Scr. **27,** 300 (1983).

Books *continued from page 1298*

wave structures.

Two closing comments: The rather brief review paper by **D. B. Ostrowsky** on Parametric Processes in $LiNbO_3$, although covering important and interesting ground, was carelessly put together, with numerous typographical errors and omissions, especially in his first two equations. The paper by **W. Horsthuis** and **R. Pannekoek** on Electrooptic Modulators in Multilayered Zinc-Oxide Waveguides demonstrates a misconception in claiming a spatially uniform electric field instrumental in coupling a symmetric mode to an antisymmetric one. By orthogonality, the overlap integral (thus the coupling coefficient) is zero if the field is uniform across the mode profiles.

I recommend this volume to any individual interested in keeping abreast of IO activity primarily in Europe and to any science library desiring completeness in its reference literature on integrated optics. These Proceedings could be regarded as complementary to the Integrated and Guided Wave Optics Conferences, such as that held in Atlanta, Georgia, in Feb. 1986, in which a greater portion of contributors represent the extensive and worthwhile efforts going on in the Western Hemisphere and Japan.

JAMES F. LOTSPEICH

Multiple Diffraction of X-Rays in Crystals. By S. CHANG. Springer-Verlag, New York, 1984. 300 pp. $36.50.

This volume—50 in the Springer Series in Solid-State Sciences—covers a phenomenon that is generally overlooked in a typical x-ray structure determination. Its incorporation in such structure determinations would surely explain some apparent discrepancies between the experimental and calculated intensities in all these determinations. However, multiple diffraction is not yet well enough understood to make its inclusion in a typical structure determination a routine matter. This, however, is not the purpose of this book. Instead Chang wishes to use the phenomenon itself as another tool to obtain information about the structure of solids. The book

continued on page 1359